JOURNAL OF SOLID STATE CHEMISTRY 60, 269–282 (1985)

Unusual Valences and Fast Electron Exchange in $MoFe_2O_4$

A. RAMDANI AND C. GLEITZER

Laboratoire de Chimie du Solide Minéral, Associé au CNRS No. 158, Université de Nancy I, B.P. 239, 54506 Vandoeuvre Les Nancy Cédex, France

G. GAVOILLE

Laboratoire d'Automatique, Université de Nancy I, France

AND A. K. CHEETHAM AND J. B. GOODENOUGH

Inorganic Chemistry Laboratory, South Parks Road, University of Oxford, Oxford OX1 3QR, United Kingdom

Received March 1, 1985

The distribution of d electrons over the cations in $MoFe_2O_4$, which is represented by the formal valence assignment, is shown to be complicated by the equilibrium reactions

$$Fe_B^{2+} + Fe_A^{3+} + Mo^{3+} \rightleftharpoons Fe_B^{3+} + Fe_A^{2+} + Mo^{3+} \rightleftharpoons Fe_B^{2+} + Fe_A^{2+} + Mo^{4+}.$$

We have used thermal treatment to confirm that the Mo are primarily on octahedral sites; $Fe_A[Mo_B Fe_B]O_4$. K-shell absorption and Mössbauer data at $T = 423$ K $> T_c$ demonstrate that the iron has an average valence near 2.5+ with fast electron transfer ($\tau_h < 10^{-8}$ sec) on both octahedral and tetrahedral sites. Paramagnetic susceptibility data give a Curie constant $C_M = 7.95 \pm 0.2$ emu/mole and a Weiss constant $\theta_p = -445$ K; magnetometer measurements confirm a compensation point near 160 K. Transport data give a surprisingly high electronic conductivity, but also give an activated mobility similar to that found in $AlFe_2O_4$ and $CrFe_2O_4$ where mixed $Fe^{3+/2+}$ valences on both A and B sites have been demonstrated. However, a positive Seebeck coefficient and a preexponential factor one order of magnitude higher in $MoFe_2O_4$ point to involvement of a fraction of the Mo atoms in electronic transport, which would be consistent with the observation of a $\tau_h < 10^{-8}$ sec on the A sites of a spinel. An energy diagram consistent with these data and other information about the relative redox potentials of these ions in oxides are proposed for this system.

Formal Valences in the Ferrospinel $MoFe_2O_4$

Introduction

In oxides, the covalent contribution to the M–O bond is certainly not negligible. Nevertheless, it is customary to refer to the filled bands that are primarily O : 2p in character as the O : $2p^6$ valence band; the bands that are primarily cationic in character are therefore designed M: d, s, or p unless there is a strong hybridization among these cationic orbitals. The band designations presented in this paper follow this convention.

0022-4596/85 $3.00

Transition-metal oxides are generally characterized by a Fermi energy E_F that lies above the top of the $O:2p^6$ valence band and below any cation–s conduction band associated with the transition metal atoms. This situation permits an unambiguous calculation of the total number of d electrons per formula unit from a knowledge of the chemical composition. However, it leaves unspecified the distribution of the electrons among the transition-metal atoms, and the assignment of formal-valence states to the transition-metal atoms represents a specification of the d electron distribution.

The following examples illustrate that specification of the d electron distribution may not be trivial:

1. $FeVO_3$. In an early investigation of this compound (*1*), it was not clear in advance whether to expect the formal valences $Fe^{2+}V^{4+}O_3$ or $Fe^{3+}V^{3+}O_3$. Cation ordering in ilmenite had established the valences $Fe^{2+}Ti^{4+}O_3$; the absence of a similar ordering in $FeVO_3$, which would convert the corundum structure to that of ilmenite, was the first indication that the correct formal valence assignment is $Fe^{3+}V^{3+}O_3$. In this compound, the first absorption band should establish the energy required for the charge transfer reaction

$$Fe^{3+} + V^{3+} \rightleftharpoons Fe^{2+} + V^{4+}. \qquad (1)$$

The activation energy must include the lattice relaxation energy, which is the solid-state analog of the reorganization energy encountered in molecular species with a change of valence. In a solid, the reorganization energy for such a reaction may be cooperative.

2. $CaFeO_3$. At room temperature, the formal iron valence in the perovskite $CaFeO_3$ is high-spin Fe^{4+}; but unlike $LaMnO_3$ (*2*), it exhibits no cooperative Jahn–Teller distortion of the Fe octahedral sites to remove the degeneracy of the ${}^5E_g$ ground configuration at lower temperatures. Rather, Mössbauer spectroscopy (*3*) has revealed a low-temperature disproportionation reaction

$$Fe^{4+} + Fe^{4+} \rightarrow Fe^{(4-\delta)+} + Fe^{(4+\delta)+} \qquad (2)$$

with $\delta \rightarrow 1$ as $T \rightarrow 0K$. The two different types of low-temperature distortions found in $LaMnO_3$ and $CaFeO_3$, which have identical numbers of d electrons per transition metal atom, have been interpreted (*4*) to signal localized σ-bonding d electrons in $LaMnO_3$, itinerant σ-bonding d electrons in $CaFeO_3$.

E. La_2CoMnO_6. Initial attempts (*5*) to prepare an ordered perovskite $La_2Co^{2+}Mn^{4+}O_6$ were frustrated by the charge-transfer reaction

$$Co^{2+} + Mn^{4+} \rightleftharpoons Co^{3+} + Mn^{3+} \qquad (3)$$

which was further complicated by a high-spin/low-spin conversion

$$Co^{3+}: t_2^4e^2 \rightleftharpoons Co^{III}: t_2^6e^0 \qquad (4)$$

that is near crossover at room temperature (*6*).

4. $LaSrCo_2O_6$. This perovskite is a metallic ferromagnet with a spontaneous magnetization corresponding to a mean cobalt moment $\mu_{Co} \simeq 1.5\ \mu_B$ (*7*). Such a fractional atomic moment cannot be rationalized either by the high-spin mixed-valent configuration $Co^{3+} + Co^{4+}$, which would have a spin-only $\mu_{Co} = 4.5\ \mu_B$, or by the low-spin configuration $Co^{III} + Co^{IV}$, which would give $\mu_{Co} = 0.5\ \mu_B$. Nor can it be rationalized by mixed high-spin and low-spin states $Co^{3+} + Co^{IV}$ or $Co^{III} + Co^{4+}$, which would give $\mu_{Co} = 2.5\ \mu_B$. However, the intermediate-spin state may be stabilized by the coexistence of itinerant σ-bonding d electrons and strongly correlated (localized) π-bonding d electrons, and this configuration gives not only the observed $\mu_{Co} \simeq 1.5\ \mu_B$, but also ferromagnetic coupling and metallic conductivity (*8*). In this case a mean cobalt valence should be designated:

$$Co^{3.5+}: t_2^5\sigma^{*0.5} \qquad (5)$$

where the σ^* band of itinerant-electron states is a d band of e-orbital parentage.

5. *Co_3O_4*. The spinel structure contains cations on both octahedral and tetrahedral sites. With two crystallographically inequivalent sites, the redox potentials for the same atom can be significantly different at the two sites. This situation is well illustrated for the normal spinel $Co^{2+}[Co_2^{III}]O_4$, which has diamagnetic low-spin $Co^{III}: t_2^6e^0$ configurations on the octahedral B sites and high-spin $Co^{2+}: e^4t_2^3$ configurations on the tetrahedral A sites. This spinel is an antiferromagnetic semiconductor with an A-site cobalt moment $\mu_{CoA} \simeq 2.7\ \mu_B$ (*9*).

6. *$Co_{3-x}Ni_xO_4$*. Nickel substitutes for octahedral-site cobalt in the system $Co_{3-x}Ni_xO_4$, and the σ-bonding electrons on tetrahedral-site cobalt and octahedral-site nickel promotes formation of a narrow band of itinerant-electron states having an equilibrium charge-transfer reaction

$$\begin{aligned} Co_A^{2+} + Ni_B^{III} &\rightleftharpoons Co_A^{III} + Ni_B^{2+} \\ e^4t_2^3 + t_2^6e^1 &\rightleftharpoons e^4t_2^2 + t_2^6e^2 \end{aligned} \qquad (6)$$

corresponding to the formal-valent configurations

$$Co_A^{(2+\delta)+}: e^4t_2^{3-\delta} + Ni_B^{(3-\delta)+}: t_2^6e^{(1+\delta)} \qquad (7)$$

where $\delta < 1$ may vary with the concentration x of nickel atoms. This situation was first established with neutron diffraction data for $Co[NiCo]O_4$ (*10*); the model was subsequently utilized to discuss the evolution of properties in the system $Co[Ni_xCo_{1-x}]O_4$ (*11*).

7. *Fe_3O_4*. Verwey (*12*) recognized early that magnetite must be an inverse spinel with Fe^{3+} ions on the A sites; a mixed valence on the B sites would then be responsible for the high electrical conductivity of this compound. His formal-valence designation $Fe^{3+}[Fe^{2+}Fe^{3+}]O_4$ implied that the mobile electrons are sufficiently localized to behave as small polarons, moving through the lattice in a diffusive motion, even though the enthalpy for an electron hop is $\Delta H_m < kT$ at room temperature. Diffusive motion requires an interatomic hopping time $\tau_h \gtrsim 10^{-13}$ sec, the period of the optical-mode vibrations. Subsequent Mössbauer data (*13*), on the other hand, have shown only an average octahedral-site valence $Fe_B^{2.5+}$, which indicates a $\tau_h < 10^{-8}$ sec. Although there is considerable evidence for a hopping-electron regime with $10^{-13} < \tau_h < 10^{-8}$ sec (*14*), whether the minority spin electrons should be considered itinerant or diffusive below the Curie temperature $T_c = 850$ K remains controversial, which makes ambiguous the proper formal-valence notation

$$Fe^{3+}[Fe^{2+}Fe^{3+}]O_4 \text{ vs } Fe^{3+}[Fe_2^{2.5+}]O_4. \qquad (8)$$

On the other hand, the energy diagram of Fig. 1 is relatively well established.

8. *$Fe_{3-x}M_xO_4$*. A significant feature of Fig. 1 is the energy required for electron transfer from a B-site Fe^{2+} ion to an A-site Fe^{3+} ion:

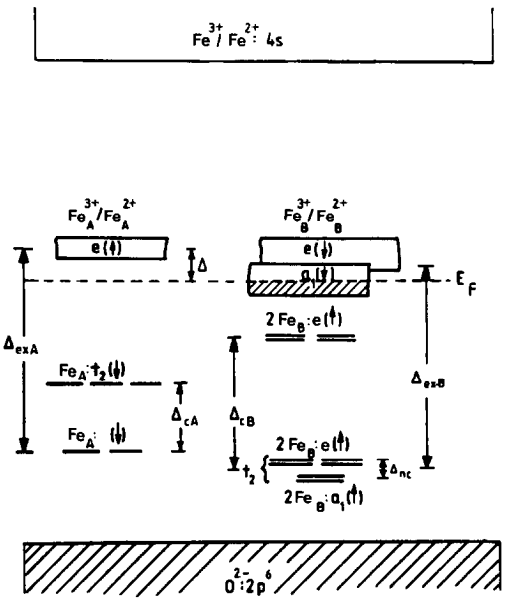

FIG. 1. Semiempirical room-temperature energy diagram for $Fe_A^{3+}[Fe_B^{2+}Fe_B^{3+}]O_4$.

$$Fe_B^{2+} + Fe_A^{3+} \rightleftharpoons Fe_B^{3+} + Fe_A^{2+} \quad (9)$$

where $\Delta G_{AB} = \Delta H_{AB} - T\Delta S_{AB}$ vanishes as $T \rightarrow 1450°C$ (15). This energy is sensitive to the introduction of substitutional ions and varies with their character and concentration. In the system $Fe[Cr_xFe_{2-x}]O_4$, for example, chromium is almost entirely confined to octahedral sites where it is stabilized in the valence state Cr^{3+}; the $Cr^{3+/2+}$ energy level lies well above the $Fe^{3+/2+}$ energy level, so the Cr^{3+} ion is not significantly reduced at normal laboratory temperatures. Therefore marked deviations from Végard's law can only be interpreted in terms of the electron transfer reaction (*9*). The variation of the lattice parameter with x at 40 K in this system (*16*), Fig. 2, can only be interpreted, therefore, as a decrease in Δ with increasing x, the value of Δ changing sign at room temperature in the compositional interval $0.5 < x < 1.2$.

In the case of $Fe[MoFe]O_4$, ambiguity about the sign and magnitude of Δ is further compounded by an uncertainty about the valence state of molybdenum:

$$Fe_B^{2+} + Fe_A^{3+} + Mo^{3+} \rightleftharpoons Fe_B^{3+} + Fe_A^{2+} + Mo^{3+} \rightleftharpoons Fe_B^{2+} + Fe_A^{2+} + Mo^{4+}. \quad (10)$$

In this paper we review previous data and report new data on this compound in an attempt to clarify the formal-valence situation.

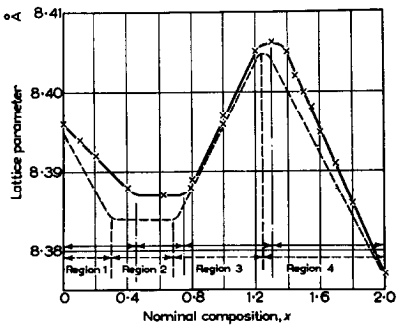

FIG. 2. Room-temperature lattice parameter versus composition for $Fe_{3-x}Cr_xO_4$ after (*16*).

TABLE I

ROOM-TEMPERATURE ISOMER-SHIFT RANGES (mm/sec wrt Fe) IN IRON OXIDES (AFTER REF. (*21*))

Coordination	Fe^{2+}	Fe^{3+}
IV	0.9–1.1	0.1–0.3
VI	1.1–1.2	0.2–0.4

Review of Previous Work

In a series of publications (*17–19*), Abe *et al.* reported the results of X-ray and neutron diffraction, magnetometer measurements, and Mössbauer spectroscopy on $MoFe_2O_4$. The cubic spinel is inverse, $Fe[MoFe]O_4$, with room-temperature lattice parameter $a_0 = 8.509$ Å and oxygen parameter $u = 0.391$. A weak magnetization (0.15–0.2 μ_B/mole) appears below a ferrimagnetic Curie temperature $T_c = 348$ K, and a compensation point is found at 160 K. These authors initially concluded that the formal valence distribution was $Fe^{2+}[Mo^{4+}Fe^{2+}]O_4$; the weak ferrimagnetic moment was attributed to unequal Fe^{2+}-ion moments on octahedral vs tetrahedral sites and/or spin canting. The molybdenum was assumed to have no magnetic moment. However, the Mössbauer spectrum showed a mean isomer shift $\delta = 0.63$ mm/sec with respect to iron at room temperature, which would indicate a mixed $Fe^{3+/2+}$ valence (see Table I), so these authors concluded in their last publication that the formal valence distribution $Fe^{3+}[Mo^{3+}Fe^{2+}]O_4$ must also be considered.

Ghose *et al.* (*20*) presented evidence for canting of the B-site spins below 70 K from neutron diffraction, magnetometer, and Mössbauer data. These authors concluded that the formal valence distribution is $Fe^{2+}[Mo^{4+}Fe^{2+}]O_4$ with a molybdenum mag-

netic moment $\mu_{Mo} \simeq 2\ \mu_B$, canting on the B-site spins accounting for the reduced molecular magnetization.

Gupta *et al.* (*21*) have examined the Mössbauer spectra principally in the paramagnetic temperature domain $T > 350$ K. They resolved the spectrum at 450 K into two doublets having isomer shifts $\delta = 0.57$ and 0.70 mm/sec with respect to iron at room temperature. They assigned these, respectively, to the iron on A and B sites. However, for both A and B sites these isomer shifts are intermediate to those anticipated for Fe^{3+} and Fe^{2+}, so these authors concluded that the formal valence distribution should be $Fe^{3+}_{0.5}Fe^{2+}_{0.5}[Mo^{3+}Fe^{2+}_{0.5}Fe^{3+}_{0.5}]O_4$, especially as such an interpretation is compatible with a relatively high electrical conductivity in this compound ($\sigma \approx 0.5 \times 10^{-2}$ Ω^{-1} cm^{-1} at room temperature). Although the formal-valence formula is written so as to indicate conduction via electron hopping ($\tau_h > 10^{-13}$ sec), nevertheless the Mössbauer spectrum could not resolve Fe^{2+} and and Fe^{3+} ions, indicating a $\tau_h < 10^{-8}$ sec as in Fe_3O_4. But in magnetite, $Fe^{3+}[Fe^{2+}Fe^{3+}]O_4$, the fast electron transfer ($\tau_h < 10^{-8}$ sec) is between B-site iron ions only; in $Fe[MoFe]O_4$ the data imply a fast electron transfer between A- and B-site iron ions as well, corresponding to a $\Delta < kT$. Fast electron transfer directly between A-site iron ions seems less probable since magnetic A–A interactions are generally weak. Moreover, the Fe^{2+} and Fe^{3+} ions on A sites in the compound $Fe^{2+}_{0.5}Fe^{3+}_{0.5}[Ni^{2+}_{0.5}Cr^{3+}_{1.5}]\ O_4$ have Mössbauer spectra that can be resolved, indicating a $\tau_h > 10^{-8}$ sec (*22*). Therefore the interpretation of Gupta *et al.* of fast electron transfer on A-site iron in $Fe[MoFe]O_4$ is of particular interest.

In the course of our study, we became aware of an additional article by Ghose (*23*) on the Mössbauer spectrum of $Fe[MoFe]O_4$ at 4 K in which he concluded, on the basis of two resolved sextuplets with internal fields of 212 and 440 kOe, that the formal valence at this temperature is $Fe^{2+}[Mo^{4+}Fe^{2+}]O_4$.

In all of the studies cited above, the samples of $MoFe_2O_4$ were prepared at high temperature (1140 and 1200°C) in H_2/CO_2 atmospheres, cooled slowly to 600°C, and then quenched. This procedure was followed because $MoFe_2O_4$ tends to decompose into $Fe_2Mo_3O_8 + Mo_xFe_{3-x}O_4$ (with $x < 1$) at temperatures $T < 400$°C; but the kinetics of the decomposition is slow at 300–400°C, and at room temperature it is too slow for any significant decomposition to occur during the lifetime of their experimental studies. However, it is important to note that in $Fe_2Mo_3O_8$, which has the structure shown in Fig. 3 (*24*), the formal valences are $Fe^{2+}_2Mo^{4+}_3O_8$ and that the Mo^{4+} ions form clusters of three edge-shared octahedra in which the Mo-4*d* electrons are spin-paired in Mo–Mo homopolar bonds (*25*).

Sample Preparation and Characterisation

A mixture of MoO_2, Fe, and Fe_2O_3 was well homogenized in an agate mortar and pressed into bar-shaped pellets. The pellets were put into an alumina crucible placed inside a silica ampule; the ampule was then degassed under vacuum and sealed under 10^{-6} Torr. The ampules were heated to 1170°C for 2 hr and then quenched. The products were black bars, and their single-phase character was verified by X-ray diffraction. The principal impurity to be anticipated, $Fe_2Mo_3O_8$, would have been easy to detect as it is well crystallized with a few characteristic lines that are strong.

A second preparation procedure was also used. A sample prepared as above was subsequently annealed at 1170°C for 12 hr in the sealed ampule; it was then slowly cooled at 25°C/hr to 600°C before quenching. The X-ray diffraction patterns of the two types of samples were identical with no variation in lattice parameter: $a_0 = 8.503$ Å, a value intermediate between those given

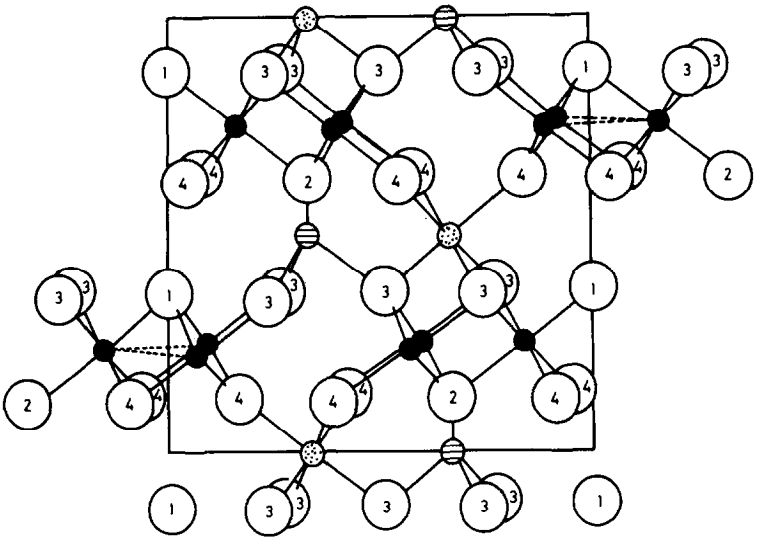

FIG. 3. The structure of $Fe_2Mo_3O_8$, after (*24*).

by Abe *et al.* (*17, 18*) and by Gupta *et al.* (*21*). The data presented below, unless otherwise specified, were taken on samples quenched from 1170°C.

In view of the strong octahedral-site preference of Mo^{3+} and Mo^{4+}, the Mo are assumed to occupy only octahedral sites. This assignment has been shown by previous workers to be applicable to samples quenched from 600°C. However, we give evidence below for a small occupancy of the A sites by molybdenum at high temperatures.

Mössbauer Data

In view of the importance of the Mössbauer analysis of Gupta *et al.* (*21*) for paramagnetic $MoFe_2O_4$ (T = 451 K), we undertook to confirm their results. This confirmation was also required because of the lack of any "criteria of quality" in their original resolution of the spectrum.

We ran spectra from 423 to 676 K; those for the quenched and slowly cooled samples were essentially identical, as can be seen from Fig. 4. The analysis in terms of two doublets, like that of Gupta *et al.*, is given in Table II for T = 423 K. (The values

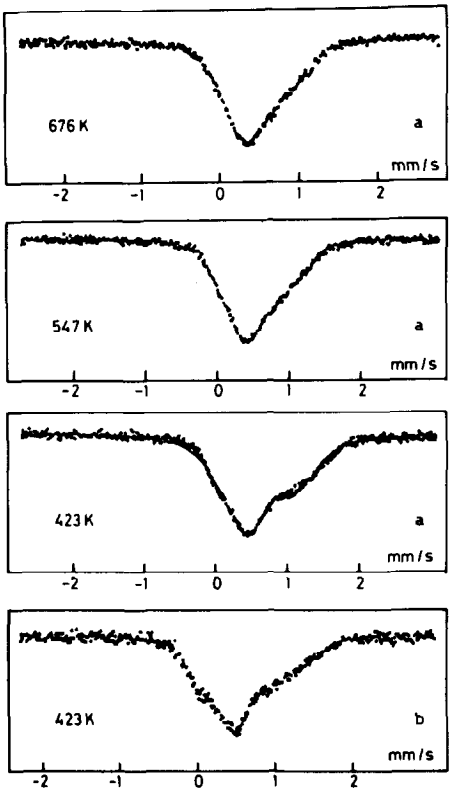

FIG. 4. Mössbauer spectra at various temperatures of $MoFe_2O_4$ (a) quenched from 1170°C and (b) slow-cooled to 600°C.

TABEL II

MÖSSBAUER ANALYSIS OF $MoFe_2O_4$ AT 423 K

Site	δ (mm/sec)	Δ (mm/sec)	Γ (mm/sec)	I	χ^2
A	0.525 (0.58)	0.22 (0.22)	0.42 (0.34)	0.42 (0.54)	2.5
B	0.65 (0.725)	0.94 (1.05)	0.56 (0.34)	0.58 (0.46)	

of Gupta *et al.* for 451 K are given in parentheses).

The calculated spectrum is shown in Fig. 4 as the continuous line in spectrum *a* for $T = 423$ *K*. The quality factor χ^2 is acceptable, but not excellent. It is typical of a compound having a statistical distribution of Mo and Fe on the B sites, which gives rise to a distribution of quadrupole splittings that enhances the widths of the resonances.

Extrapolation of the isomer shifts to 300 K and correction for the second-order Doppler shift (*26*) gives $\delta_A \approx 0.62$ and $\delta_B \approx 0.75$ mm/sec, values characteristic of a mixed valence on the iron with a mean valence state of about +2.5 and $\tau_h < 10^{-8}$ sec (see Table I).

Even without a resolution of the spectrum into contributions from A and B sites, the center of gravity of the spectrum—calculated from the raw data without interpretation—occurs at a $\delta = 0.62$ mm/sec, which extrapolates to 0.70 mm/sec at room temperature. This value is characteristic of a mixed-valence compound with a mean iron valence of about +2.5. These results thus establish the fact that, at least in the paramagnetic state, the molybdenum has a formal valence close to, if not precisely, Mo^{3+}.

On the assumption that the recoil-free fractions of the two sites are the same, Mössbauer analysis gives an intensity ratio $I_B/I_A = 1.38$, which suggests that some of the molybdenum atoms occupy A sites in samples quenched from 1170°C. This deduction is marginally supported by analysis of neutron diffraction data as well as the observation that the magnetic properties depend in a small, but indisputable, manner on the thermal treatment of the sample.

Finally it should be noted that resolution of the Mössbauer spectrum into two doublets that reflect not only the two different types of sites, but also a distribution of Fe^{3+} ions on A sites and Fe^{2+} ions on B sites, gives a plausible solution with the same quality factor χ^2. In either interpretation, the molybdenum has a formal valence close to Mo^{3+}. With this latter interpretation, the relatively high electronic conductivity—see below—would be due to Mo–Mo interactions on the B sites giving rise to amorphous band delocalization (as against metal–metal clustering); the Mo concentration exceeds the percolation limit. However, the equilibrium constant $[Fe_A^{3+}][Fe_B^{2+}]/[Fe_A^{2+}][Fe_B^{3+}]$ corresponds to an enthalpy of only −4 kcal/mole at 900°C (*27*), which indicates that Δ is too small for the minority spin electron on the iron atoms to be restricted to one subarray in the paramagnetic region.

Magnetic Measurements

The room-temperature magnetization σ_m in applied field H is shown in Fig. 5; the magnetization at 5950 Oe vs temperature T is shown in Fig. 6 for the temperature interval $100 < T < 500$ K. It is to be noted that at room temperature σ_m is essentially saturated at 5950 Oe and is close to its maximum value in Fig. 6. Also shown in Fig. 6

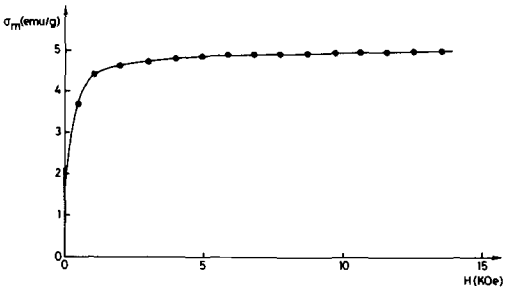

FIG. 5. Magnetization σ_m of $MoFe_2O_4$ versus field H at 296 K.

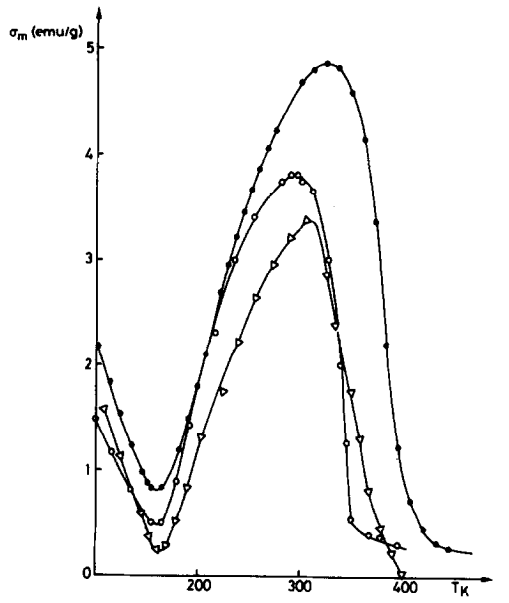

FIG. 6. Magnetization σ_m of $MoFe_2O_4$ versus temperature T in an applied field of 5950 Oe. Comparable curves by (*18*) (–O–, H_{app} = 7520 Oe) and (*20*) (–▽–, H_{app} = 1 T) are also shown.

are the σ_m vs T curves obtained by previous workers. The curves are all similar, each showing a maximum near room temperature and a compensation point near 160 K. These curves were taken on a sample slow-cooled to 600°C, as were the samples investigated by previous workers. The principal difference between our specimen and those of previous workers is a somewhat larger Curie temperature T_c. A sample quenched from 1170°C gave a similar σ_m vs T curve, but with a slightly lower compensation point. This result seems to indicate that the Mo-atom distribution is not significantly altered by the different thermal treatments employed in this study.

Figure 7 shows the first magnetization cycle at 4.2 K for a sample cooled in the absence of an applied magnetic field. At this temperature, σ_m is not saturated in an applied field approaching 2 T, and the magnetization is only about 0.1 μ_B/mole. Moreover, the coercive force is high, and the hysteresis loop exhibits a significant "trainage," saturation being more difficult to achieve on the initial magnetization curve. Similar curves were reported by Ghose *et al.* (*20*). This behavior is typical of a spin glass, and no reliable information about the valence distribution can be deduced from the magnitude of σ_m.

No previous attempt has been made to measure the paramagnetic susceptibility as a function of temperature because of the decomposition of the phase in the neighborhood of 400°C. However, we have found that heating at 300°C/hr is rapid enough to obtain reproducible results without any X-ray evidence for the separation of a second phase, provided the temperature does not exceed 900 K. The susceptibility data (Fig. 8) are typical for a ferrimagnet, and the high-temperature values approach a Curie–Weiss law with a Curie constant C_M = 7.95 ± 0.2 emu/mole and a Weiss constant of $\theta_p = -445$ K.

The large, negative Weiss constant is typical for an antiferromagnetic Fe_A–O–Fe_B superexchange interaction; the Curie temperature (≈ 400 K) is of somewhat smaller magnitude than the 713 K of $MgFe_2O_4$ (*28*) and larger than the 120 K of $TiFe_2O_4$ (*29*). In $MgFe_2O_4$ the Fe_A–O–Fe_B interactions are between Fe^{3+} ions, in $TiFe_2O_4$ they are between Fe^{2+} ions. Thus

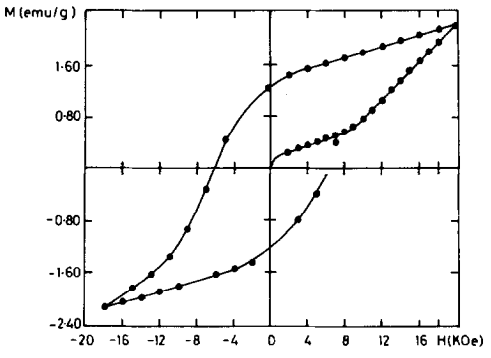

FIG. 7. Initial magnetization and first hysteresis loop of $MoFe_2O_4$ at 4.2 K.

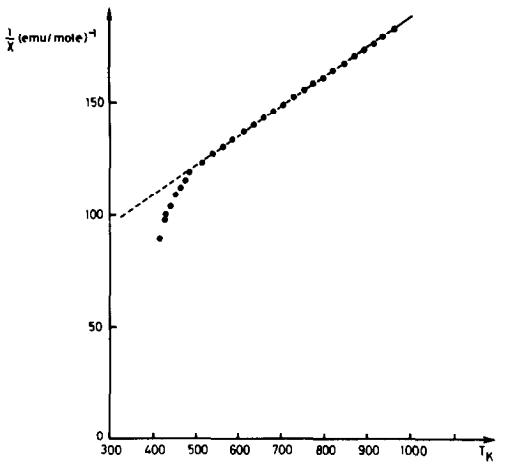

FIG. 8. Temperature dependence of the inverse paramagnetic susceptibility of $MoFe_2O_4$.

the magnitude of the Curie temperature is consistent with a mixed $Fe^{3+/2+}$ valence in $MoFe_2O_4$.

The molybdenum may or may not contribute to the temperature dependence of the paramagnetic susceptibility. Since each Mo atom has, on average, three nearest-neighbor Mo in nearest-neighbor octahedral sites sharing octahedral-site edges, the Mo–Mo interactions are expected to be strong enough to suppress the formation of localized atomic moments on most, if not all, of the molybdenum atoms. A fast ($\tau_h < 10^{-8}$ sec) electron transfer between iron atoms of a mixed-valent configuration, as deduced from the Mössbauer data, would substantially reduce the orbital contribution to the iron atomic moment, so we can compare the experimental Curie constant with the spin-only values of Table III, which were calculated for various formal-valence distributions. The iron atoms are all high-spin; an improbable low-spin configuration of the Mo atoms (the octahedral sites are distorted in the spinel to trigonal symmetry) is included for completeness.

The measured value $C_M = 7.95$ emu/mole is more compatible with a formal valence Mo^{3+} than Mo^{4+}, especially as the molybdenum atoms are not expected to contribute a full localized electron moment. Any localized moments on Mo^{4+} ions would introduce a strong magnetic anisotropy even at room temperature, which is not observed (Fig. 5). Therefore the magnetic susceptibility data points to a Mo^{3+} valence state in $MoFe_2O_4$, but with little contribution to the temperature-dependent part of the susceptibility from the Mo^{3+} ions. In the absence of a Mo^{3+}-ion contribution, a spectroscopic splitting factor $g \approx 2.3$ would need to be invoked, which would reflect a quite reasonable orbital contribution, especially with a high concentration of high-spin Fe^{2+} ions.

Electrical Measurements

In Fig. 9, the temperature dependence of the electrical conductivity of polycrystalline $MoFe_2O_4$ is compared with the conductivities of polycrystalline $AlFe_2O_4$, $Al_{1.8}Fe_{1.2}O_4$, and $CrFe_2O_4$, all measured by us under the same conditions. In all samples, two changes of slope in log (σT) vs T^{-1} are observed; one occurs approximately at the Curie temperature, the other at a lower temperature. The high-temperature break reflects the common higher activation energy for a mixed-valence electron transfer above a magnetic-ordering temperature. The low-temperature break may be associated with a freezing of the phonon spectrum that occurs near $\theta_D/2$, which leads to a De-

TABLE III

CALCULATED SPIN-ONLY CURIE CONSTANTS FOR DIFFERENT ELECTRON CONFIGURATIONS OF MOLYBDENUM

Mo^{4+}	C_M (emu/mole)	Mo^{3+}	C_M (emu/mole)
$t_2^2e^0$	7.0	$t_2^3e^0$	9.25
$a_1^2e_\pi^0e_\sigma^0$	6.0	$a_1^2e_\pi^1e_\sigma^0$	7.75
Itinerant	6.0	Itinerant	7.4

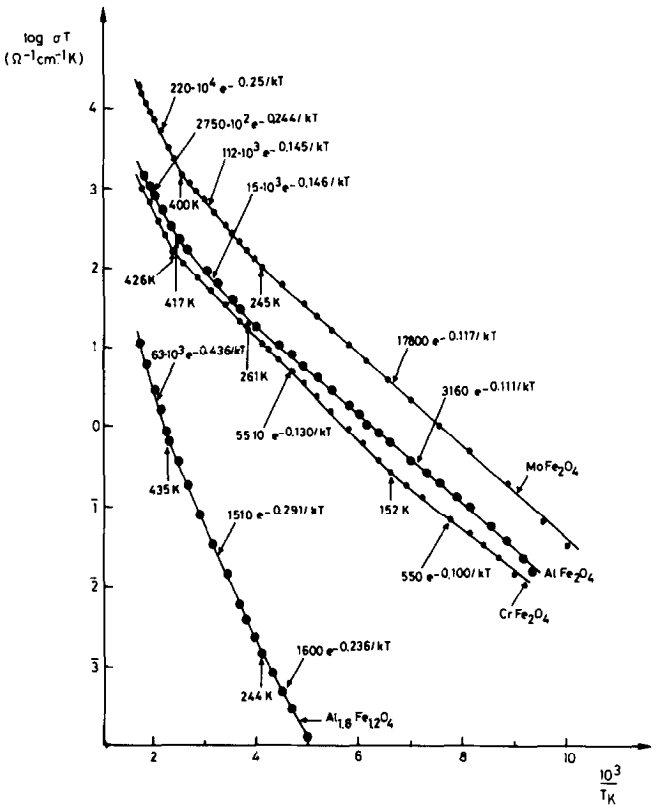

FIG. 9. Temperature dependence of the electrical conductivity σ, plotted as log (σT) vs T^{-1}, for MFe_2O_4, (M = Mo, Cr, Al) and $Al_{1.8}Fe_{1.2}O_4$.

bye temperature $\theta_D \approx 490$ K for $MoFe_2O_4$, a reasonable value for a ferrospinel.

Of particular interest for the present discussion is the fact that the electrical conductivity of $MoFe_2O_4$ is roughly a factor of 10 higher than the conductivities of the two known mixed-valent compounds $AlFe_2O_4$ and $CrFe_2O_4$. In $Al_{1.8}Fe_{1.2}O_4$, the concentration of trivalent iron is greatly reduced and tends to be associated with A-site iron; the conductivity is therefore also greatly reduced.

Although the concentration of molybdenum in $MoFe_2O_4$ exceeds the percolation limit for electrical conduction via Mo–Mo pathways, the comparable slopes of the log (σT) vs T^{-1} curves for $MoFe_2O_4$, $CrFe_2O_4$, and $AlFe_2O_4$ imply a similar conduction mechanism in all three compounds. In the spinels $Fe[Cr^{3+}Fe]O_4$ and $Al_\delta Fe_{1-\delta}[Al_{1-\delta}Fe_{1+\delta}]O_4$, conduction is via a mixed $Fe^{3+/2+}$ valence in both A and B sites, which gives rise to mobile small polarons on the B sites (*4*). In $MoFe_2O_4$, the activation energy in the small polaron mobility appears to be comparable, but the preexponential factor is increased by an order of magnitude. This factor is proportional to $Nc(1-c)\nu_o \exp(\Delta S_m/k)$, where the attempt frequency ν_o should be little altered. A change in the concentration c of mobile charge carriers on N energetically equivalent lattice sites per unit valence cannot account, by itself, for the enhancement of the preexponential factor, and there is little basis for expecting a marked change in the motional entropy ΔS_m unless the density N of energetically equivalent sites is significantly larger. Thus

the conductivity data points to a small polaron conduction mechanism in Fe[Mo Fe]O_4 in which nearly all the cation sites Fe_A, Fe_B, and Mo_B may be considered energetically equivalent as implied by the formal-valence equilibrium relationships of Eq. (10).

The thermoelectric power offers a check on this radical hypothesis. We measured a room-temperature Seebeck coefficient of 24 $\pm$ 3 μV/d° that decreased only slightly with temperature to 300°C. A nearly temperature-independent Seebeck coefficient implies that the activation energy in the electrical conductivity is primarily due to an activated mobility in a mixed-valent configuration. In such a case, the Seebeck coefficient is given by

$$\theta \approx -(k/e)\ln[\beta(1 - c)/c] \qquad (11)$$

where β is the spin degeneracy factor. The concentration of mobile carriers c depends upon the formal valence assignments and on the density of sites that are considered energetically equivalent, as can be seen from Table IV.

If mobile electrons have equal access to all cations, the limiting value of c is $c = \frac{2}{3}$ corresponding to a formal valence $Fe_\alpha^{3+}Fe_{1-\alpha}^{2+}[Mo_{1-2\alpha}^{4+}Mo_{2\alpha}^{3+}Fe_\alpha^{3+}Fe_{1-\alpha}^{2+}]O_4$, $\alpha = \frac{1}{3}$. Even for a spin degeneracy factor $\beta = 1$, which we adopt in the absence of any sharp rise in θ with increasing temperature through T_c, the magnitude of the measured Seebeck coefficient corresponds to an effective $c \approx 0.57$, which is significantly smaller than the limiting value of $c = 0.67$. This result can be interpreted in two ways:

TABLE IV

THE CONCENTRATION c MOBILE CHARGE CARRIERS FOR VARIOUS FORMAL VALENCE SITUATIONS IN Fe[MoFe]O_4

2[4,2]	3[3,2]	2[$\frac{4}{3}$,$\frac{2}{3}$]; $\frac{2}{3}$[3,$\frac{2}{3}$]	$\frac{2}{3}$[$\frac{4}{3}$,$\frac{2}{3}$]
c: 0 or 1	Activated	$\frac{1}{2}$	$\frac{2}{3}$

TABLE V

K-SHELL ABSORPTION EDGES IN THE PHOTON ENERGY RANGE 5–20 eV

Compound		Transition energies (eV)		
$CrFe_2O_4$		10.4	15.1	19.7
	(5.2)[a]	(9)	(12.8)	(17.8)
$AlFe_2O_4$		Shoulder	14.4	19.4
		(8.6)	(12.2)	(17.4)
$MoFe_2O_4$		Shoulder	14.2	19.1
	(5)	(8.6)	(11.7)	(17.3)

[a] Calculated values are in parentheses.

(1) The mobile electrons have nearly equal access to both A and B sites and to a fraction of the Mo_B atoms. (2) All molybdenum are Mo_B^{3+}, and hence inaccessible to the mobile electrons, but a $\Delta > 0$ enhances the Fe_B^{2+}-ion concentration relative to the Fe_A^{2+}-ion concentration and the B-site conduction alone is responsible for the sign of θ, as established in several other spinels (*30*), despite an A–B electron-equilibrium exchange. The latter interpretation cannot account for the enhanced conductivity in $MoFe_2O_4$ compared to $AlFe_2O_4$ and $CrFe_2O_4$.

K-Shell Absorption Spectra

The *K*-shell absorption edge of an element depends primarily on its degree of oxidation and anion coordination. Moreover, the time to excite an electron is short compared to τ_h for a small polaron, so the different valences of a mixed-valence state are revealed. Table V shows data of Lenglet *et al.* (*31*) for the *K*-shell absorption edges, as normally defined, of $MoFe_2O_4$, $AlFe_2O_4$, and $CrFe_2O_4$. The sample of $MoFe_2O_4$ was supplied by us, so it was prepared under the same conditions as the samples reported on above.

Both $AlFe_2O_4$ and $CrFe_2O_4$ contain mixed Fe^{3+} and Fe^{2+} valences on both A and B sites (*4*). The similarity of their spectra to the spectrum of $MoFe_2O_4$ confirms

that the iron has a mixed valence on both tetrahedral and octahedral sites of Mo Fe_2O_4 and therefore that the molybdenum is at least partially, if not completely, reduced to the Mo^{3+} state.

Discussion

The Mössbauer spectrum at 420 K, the high electrical conductivity, the paramagnetic susceptibility, and the *K*-shell absorption spectrum all point unambiguously to a mixed $Fe^{3+/2+}$ valence on both the tetrahedral A and octahedral B sites; the molybdenum must therefore be primarily in the trivalent Mo^{3+} state, but without making an important contribution to the paramagnetic susceptibility. Moreover, the mobile charge carriers appear to have an activated mobility, indicating they are small polarons ($\tau_h > 10^{-13}$ sec), even though the Mössbauer spectrum appears to have a mean $Fe^{3+/2+}$ isomer shift for both the A and B sites, which indicates a $\tau_h < 10^{-8}$ sec. On the other hand, the positive Seebeck coefficient is incompatible with a formal-valence distribution $Fe^{2+}_{0.5}Fe^{3+}_{0.5}[Mo^{3+}Fe^{2+}_{0.5}Fe^{3+}_{0.5}]O_4$. Either the B sites are Fe^{2+}-ion-rich and the sign of the Seebeck coefficient is determined by only the B-site charge transfer, or some of the Mo^{3+} are oxidized to Mo^{4+}.

At low temperatures, an antiferromagnetic component to the B-site moment, whether due to canting or to an antiferromagnetic coupling of any Mo-atom moments, is incompatible with a ferromagnetic double-exchange interaction due to mobile B-site electrons. Finally, the observation of Mo^{4+} ions coexisting on octahedral sites with Fe^{2+} ions in $Fe_2Mo_3O_8$, a phase into which $MoFe_2O_4$ disproportionates at intermediate temperatures, would seem to argue against the stabilization of Mo^{3+} ions in the presence of mixed-valent $Fe^{3+/2+}$ configurations on both octahedral and tetrahedral sites. Our problem is to reconcile these observations.

The fact that the energy of Δ of Fig. 1 passes through zero at room temperature in the system $Fe_{3-x}Cr_xO_4$ at $x \approx 0.9$ (see Fig. 2) demonstrates that $\Delta < kT$ in $MoFe_2O_4$ is more probable than improbable. The $Mo^{4+/3+}$ ion, like the Cr^{3+} ion, has empty σ-bonding *d* orbitals, the *e* orbitals of an octahedral site cation, and can be expected to influence Δ in a manner similar to that of the Cr^{3+} ion.

In the compound $Fe_2Mo_3O_8$, the Mo^{4+} ions are ordered into triangular clusters of edge-shared octahedra. In this configuration, each Mo atom has two nearest-neighbor Mo atoms with two Mo–Mo bond angles at 60° to one another. A strong trigonal component to the crystalline field splits the octahedral site threefold-degenerate t_2 manifold into twofold-degenerate e_π and nondegenerate a_1 orbitals. The e_π orbitals are nearly coplanar and are rotated by 60° with respect to each other. Therefore the two e_π orbitals form Mo–Mo bonding and antibonding molecular orbitals within a triangular cluster that are split by a finite energy gap; the bonding states are filled and stabilized relative to the a_1 orbital, which experiences only the Mo–O antibonding reaction. Therefore the Mo^{4+} ions are diamagnetic, and the compound is semiconducting primarily because there is an energy gap between the filled, bonding e_π states of a Mo_3^{4+} cluster and the a_1 energies. Any correlation splitting between Mo^{4+} and Mo^{3+} states must be small; the metallic character of the perovskite $CaMoO_3$ demonstrates that this correlation splitting is less than the bandwidth (*6*). However, what has not been established are the relative energies of the minority-spin electron on the high-spin Fe^{2+} ion and the empty a_1 orbital on the Mo^{4+} ions.

In the ordered perovskites A_2FeMoO_6 (*A* = Ba, Sr, or Ca), the coexisting octahedral-site ions have the formal valences Fe^{3+} and Mo^{5+} rather than Fe^{2+} and Mo^{6+} (*6*), which places the $Fe^{3+/2+}$ redox couple above the $Mo^{6+/5+}$ couple. On the other hand, the

Fe^{2+} ion does not reduce tetrahedral-site Mo^{6+} in $FeMoO_4$ (*32*). Therefore, the finding of a coexistence of Mo^{3+} and Fe^{2+} ions in the spinel $MoFe_2O_4$ must be considered an unexpected result, and we should not anticipate the $Mo^{4+/3+}$ couple to lie at a significantly lower energy than the two $Fe^{3+/2+}$ couples. In fact, if the $Mo^{4+/3+}$ energies are spread over a bandwidth of any magnitude, we should expect an overlap of the $Mo^{4+/3+}$ band and the localized $Fe^{3+/2+}$ energy levels. It remains to argue that we must anticipate a $Mo^{4+/3+}$ bandwidth of several eV and why its center may lie below the $Fe^{3+/2+}$ levels in the spinel $MoFe_2O_4$.

We have already pointed out that the Mo^{4+} ion exhibits strong Mo–Mo interactions across shared octahedral-site edges in $Fe_2Mo_3O_8$ and strong Mo–O–Mo interactions in $CaMoO_3$. In MoO_2, which has the distorted rutile structure, strong Mo–Mo interactions across shared octahedral-site edges caused Mo–Mo dimerization and strong Mo–O–Mo interactions give rise to metallic conductivity (*25*). None of these molybdenum compounds exhibits a spontaneous magnetic moment on the molybdenum ions, indicating that any tendency to correlation splitting is suppressed by stronger Mo–Mo interactions.

In $MoFe_2O_4$, each octahedral site Mo has, on the average, three Mo nearest neighbors sharing a common octahedral site edge. However, the Mo atoms are statistically distributed over the octahedral sites, so some Mo atoms will have more and some less than three Mo nearest neighbors. Moreover, the nearest octahedral-site neighbors are so arranged in the spinel structure that each of the t_2 orbitals of octahedral site symmetry is directed toward a nearest neighbor. In $Ga_{0.5}[Mo_2]S_4$, the Mo atoms form tetrahedral clusters, indicating strong Mo–Mo interactions within the thiospinel framework $[Mo_2]S_4$ (*25*), and stronger Mo–Mo interactions can be expected within an oxospinel framework. These strong interactions must significantly reduce any correlation splitting between $Mo^{5+/4+}$ and $Mo^{4+/3+}$ couples, thereby making the Mo^{4+} valence state accessible to reduction by an Fe^{2+} ion if it has three nearest-neighbor Mo in positions that can bond with each of its three t_2 orbitals. However, the statistical distribution of Mo atoms over the octahedral sites gives Mo–Mo bonding more like that in an amorphous solid, so the $Mo^{4+/3+}$ band should be broadened by "wings" extending beyond a mobility edge (*33*), but with is center of gravity at or below the $Fe^{3+/2+}$ redox energies for the solid. The energy diagram of Fig. 1 thus becomes modified by the addition of such a band, as shown in Fig. 10, and by a $\Delta < kT$. Electrons in states above the mobility edge can contribute localized spins and hence to the Curie constant.

Since the Mo concentration is high enough to exceed the percolation limit, we must anticipate metallic conduction if the Fermi energy lies below the mobility edge in the $Mo^{4+/3+}$ band of $MoFe_2O_4$. The fact that small-polaron conduction is observed places the Fermi energy above any mobility edge, and therefore some localized spins may be associated with the Mo array. Localized states at the bottom of the $Mo^{4+/3+}$

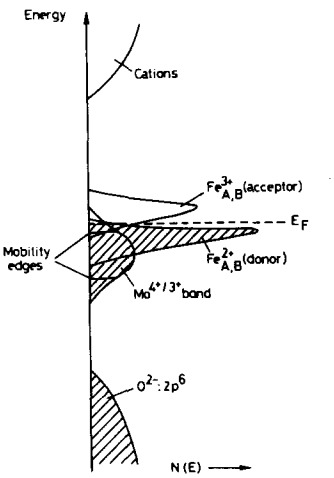

FIG. 10. Proposed energy diagram for $MoFe_2O_4$.

band would contain spin-paired electrons in Mo–Mo bonds, so they are not expected to contribute localized spins. Thus the model is consistent with a small Mo-atom contribution to the magnetic susceptibility. Moreover, the observation of (i) a coercive force that is high at low temperatures and low at high temperatures, (ii) a compensation point, and (iii) a spin glass behavior at low temperature is consistent with a high anisotropy on the spins localized at Mo atoms, this anisotropy effect being analogous to that observed in the spinel Co_2TiO_4 (*34*). At low temperatures, these ions would be decoupled from any double exchange component of the magnetic exchange; at these temperatures the activation energy in the mobility lengthens the hopping time τ_h to beyond the length of the spin relaxation time.

In conclusion, Fig. 10 offers a qualitative model for the interpretation of the physical properties of $MoFe_2O_4$. It confronts the problem of formal valence posed in Eq. (10).

Acknowledgment

The authors are grateful to Professor M. Lenglet (University of Rouen) for kindly providing the data on *K*-shell absorption.

References

1. J. B. GOODENOUGH, "Magnetism and the Chemical Bond," p. 104, Interscience Wiley (1963).
2. J. B. GOODENOUGH, *Phys. Rev.* **100,** 564 (1955).
3. M. TAKANO, N. NAKANISHI, Y. TAKEDA, S. NAKA, AND T. TAKADA, *Mater. Res. Bull.* **12,** 923 (1977).
4. C. GLEITZER AND J. B. GOODENOUGH, *Struct. Bonding (Berlin)* **61,** 1 (1985).
5. J. B. GOODENOUGH, A. WOLD, R. J. ARNOTT, AND N. MENYUK, *Phys. Rev.* **124,** 373 (1961).
6. J. B. GOODENOUGH AND J. M. LONGO, "Landolt–Bornstein Tabellen New Series," Vol. III/4a, 126 (1970).
7. G. H. JONKER AND J. H. VAN SANTEN, *Physica* **19,** 120 (1953).
8. J. B. GOODENOUGH, *Mater. Res. Bull.* **6,** 967 (1971).
9. C. INFANTE, D. Phil. Thesis, Oxford (1975).
10. P. D. BATTLE, A. K. CHEETHAM, AND J. B. GOODENOUGH, *Mater. Res. Bull.* **14,** 1013 (1979).
11. J. A. K. TAREEN, A. MALECKI, J. P. DOUMERC, J. C. LAUNAY, P. DORDOR, M. POUCHARD, AND P. HAGENMULLER, *Mater. Res. Bull.* **19,** 989 (1984).
12. E. J. W. VERWEY, *Nature (London)* **144,** 327 (1939); E. J. W. Verwey and P. W. Haaymann, *Physica* **8,** 979 (1941).
13. G. A. SAWATZKI, J. M. D. COEY, AND A. MORRISH, *J. Appl. Phys.* **40,** 1402 (1969).
14. J. B. GOODENOUGH, "Recent Advances in Materials Research" (C. M. Srivastava, Ed.) pp. 4–20, Oxford and IBH Publ. Co., New Delhi (1984).
15. C. WU AND T. O. MASON, *J. Amer. Ceram. Soc.* **64,** 520 (1981).
16. M. H. FRANCOMBE, *J. Phys. Chem. Solids* **3,** 37 (1957).
17. M. ABE, M. KAWACHI, AND S. NOMURA, *J. Phys. Soc. Japan* **31,** 940 (1971).
18. M. ABE, M. KAWACHI, AND S. NOMURA, *J. Phys. Soc. Japan* **33,** 1296 (1972).
19. M. ABE, M. KAWACHI, AND S. NOMURA, *J. Phys. Soc. Japan* **34,** 565 (1973).
20. J. GHOSE, N. N. GREENWOOD, A. C. HALAM, AND D. A. READ, *J. Solid State Chem.* **11,** 239 (1974).
21. M. GUPTA, S. KANETKAR, S. DATE, A. NIGAKEVAR, AND A. SINHA, *J. Phys. C* **12,** 2401 (1979).
22. R. GERARDIN, A. RAMDANI, C. GLEITZER, B. GILLOT, AND B. DURAND, *J. Solid State Chem.* **57,** 215 (1985).
23. J. GHOSE, *Hyperfine Interact.* **15/16,** 755 (1983).
24. G. B. ANSELL AND L. KATZ, *Acta Crystallogr.* **21,** 482 (1966).
25. J. B. GOODENOUGH, "Proc. Climax 4th Int. Conf. Chemistry and Uses of Molybdenum" (H. F. Barry and P. C. M. Mitchell, Eds.) pp. 1–22, Climax Molybdenum Co., Ann Arbor, Mich. (1982).
26. R. IRALDI, G. LE CAER, AND C. GLEITZER, *Solid State Commun.* **40,** 145 (1981).
27. K. FITZNER, *Thermochim. Acta* **31,** 227 (1979).
28. L. M. CORLISS, J. M. HASTINGS, AND F. G. BROCKMAN, *Phys. Rev.* **90,** 1013 (1953).
29. S. AKIMOTO, T. KATSURA, AND M. YOSHIDA, *J. Geomagn. Geolect. (Japan)* **9,** 165 (1957).
30. A. TRESTMAN-MATTS, S. DORRIS, S. KUMARAKRISHNAN, AND T. MASON, *J. Amer. Ceram. Soc.* **66,** 829 (1983).
31. M. LENGLET *et al.* (in press).
32. A. SLEIGHT, B. CHAMBERLAND, AND J. WEIBER, *Inorg. Chem.* **7,** 1093 (1968).
33. N. F. MOTT AND E. A. DAVIS, "Electonic Processes in Non-crystalline Materials," Oxford Univ. Press (Clarendon), London/New York (1979).